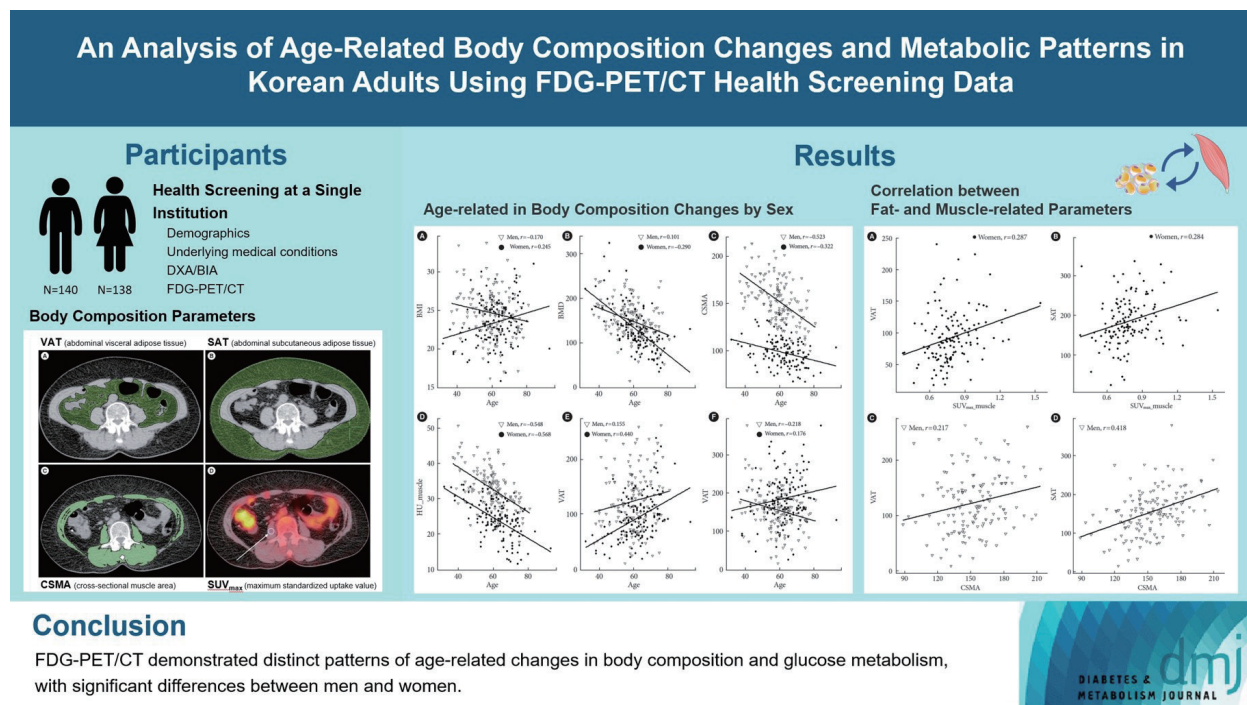


# An Analysis of Age-Related Body Composition Changes and Metabolic Patterns in Korean Adults Using FDG-PET/CT Health Screening Data

Chang-Myung Oh, Ji-In Bang, Sang Yoon Lee, Jae Kyung Lee, Jee Won Chai, So Won Oh

Diabetes Metab J Published online Sep 2, 2024 | <https://doi.org/10.4093/dmj.2024.0057>



## Highlights

- The FDG-PET/CT scan accurately quantifies body composition and glucose metabolism.
- Age-related changes in bone density, muscle mass, and fat differ significantly by sex.
- Glucose metabolism is closely linked to fat quantity, distribution, and metabolic conditions.

## How to cite this article:

Oh CM, Bang JI, Lee SY, Lee JK, Chai JW, Oh SW. An Analysis of Age-Related Body Composition Changes and Metabolic Patterns in Korean Adults Using FDG-PET/CT Health Screening Data. Diabetes Metab J Published online Sep 2, 2024. <https://doi.org/10.4093/dmj.2024.0057>

# An Analysis of Age-Related Body Composition Changes and Metabolic Patterns in Korean Adults Using FDG-PET/CT Health Screening Data

Chang-Myung Oh<sup>1,\*</sup>, Ji-In Bang<sup>2,\*</sup>, Sang Yoon Lee<sup>3</sup>, Jae Kyung Lee<sup>4</sup>, Jee Won Chai<sup>5</sup>, So Won Oh<sup>6</sup>

<sup>1</sup>Department of Biomedical Science and Engineering, Gwangju Institute of Science and Technology, Gwangju,

<sup>2</sup>Department of Nuclear Medicine, CHA Bundang Medical Center, CHA University, Seongnam,

Departments of <sup>3</sup>Rehabilitation Medicine, <sup>4</sup>Internal Medicine, <sup>5</sup>Radiology, <sup>6</sup>Nuclear Medicine, Seoul Metropolitan Government Seoul National University Boramae Medical Center, Seoul, Korea

**Background:** F-18-fluorodeoxyglucose positron emission tomography (FDG-PET)/computed tomography (CT) can be used to measure bone mineral density (BMD), cross-sectional muscle area (CSMA), Hounsfield units (HU) of liver and muscle, subcutaneous adipose tissue (SAT), abdominal visceral adipose tissue (VAT), and glucose metabolism. The present study aimed to identify age-related changes in body composition and glucose metabolism in Korean using opportunistic FDG-PET/CT imaging.

**Methods:** We analyzed FDG-PET/CT, clinical history, and laboratory data abstracted from the medical records of patients who underwent health screening at a single institute between 2017 and 2022.

**Results:** In total, 278 patients were included in the analysis (male:female = 140:138). Age and body mass index were positively correlated in female, but negatively correlated in male. BMD decreased with age more in female, and CSMA decreased with age more in male. Muscle HU decreased with age for both sexes. In female, SAT and VAT increased with age; and in male, SAT decreased slightly while VAT remained stable. Muscle glucose metabolism showed no association with age in male but increased with age in female. CSMA correlated positively with BMD overall; and positively correlated with VAT and SAT in male only. In female only, both SAT and VAT showed negative correlations with glucose metabolism and correlated positively with muscle glucose metabolism. Liver HU values were inversely correlated with VAT, especially in female; and positively correlated with muscle glucose metabolism in female only.

**Conclusion:** FDG-PET/CT demonstrated distinct patterns of age-related changes in body composition and glucose metabolism, with significant differences between sexes.


**Keywords:** Aging; Body composition; Positron emission tomography computed tomography

## INTRODUCTION

Cross-sectional body imaging, such as computed tomography (CT), acquired during health screening or other medical examinations, provides comprehensive and objective data on internal tissues and organs. CT can be used to quantify various parameters, including bone mineral density (BMD), fat mass of visceral adipose tissue (VAT) and subcutaneous adipose tis-

sue (SAT), fat content in the skeletal muscle and liver, and arterial vascular calcifications [1,2]. Body composition data that is opportunistically acquired or incidentally obtained during clinical imaging—referred to as “opportunistic screening”—can provide valuable, objective information which can contribute to the assessment of an individual’s overall health and the identification of various health conditions [3].

Opportunistic body composition analysis in the context of

Corresponding author: So Won Oh  <https://orcid.org/0000-0001-8967-8923>  
Department of Nuclear Medicine, Seoul Metropolitan Government Seoul National University Boramae Medical Center, 20 Boramae-ro 5-gil, Dongjak-gu, Seoul 07061, Korea  
E-mail: mdoosw@snu.ac.kr

\*Chang-Myung Oh and Ji-In Bang contributed equally to this study as first authors.

Received: Feb. 15, 2024; Accepted: Apr. 24, 2024

This is an Open Access article distributed under the terms of the Creative Commons Attribution Non-Commercial License (<https://creativecommons.org/licenses/by-nc/4.0/>) which permits unrestricted non-commercial use, distribution, and reproduction in any medium, provided the original work is properly cited.

aging has garnered significant attention from researchers over recent years [1-4]. The aging process induces a multitude of physiological alterations, including reduction in bone density, decline in muscle mass, and increase in fat mass; precipitating discernible changes in the overall body composition [5,6]. These changes are intricately interconnected, and collectively exert potential effects on the health and overall quality of life of elderly individuals [7,8]. The concept of aging-well focuses on promoting healthy aging, maintaining functional autonomy, and enhancing the quality of life of the older population [9]. In the current global era characterized by a demographic shift toward an aging society, the importance of aging-well is becoming more important than ever.

F-18-fluorodeoxyglucose positron emission tomography (FDG-PET) is a pivotal imaging modality which provides functional information about various tissues and organs, and can be complemented by the integration of body composition data from CT. As such, FDG-PET/CT is a versatile tool for quantifying various parameters, encompassing the quantity and distribution of adipose tissue, quantity and quality of skeletal muscles, bone density, and glucose metabolism of various tissues. The objective of the present study was to analyze body composition and glucose metabolism related to aging in Korean adults undergoing FDG-PET/CT for health screening.

## METHODS

### Study population

We conducted a retrospective analysis of all patients who underwent FDG-PET/CT imaging for health screening at a single major metropolitan hospital in South Korea between January 2017 and 2022. Comprehensive data, including body weight, height, and blood glucose levels at the time of FDG injection were collected for each patient. Body mass index (BMI) was calculated as the ratio of body weight to the square of height in meters ( $\text{kg}/\text{m}^2$ ). In alignment with the Korean guidelines, abdominal obesity was defined as a waist circumference (WC) of 90 cm or greater in male and 85 cm or greater in female [10]. Information about underlying medical conditions, including type 2 diabetes mellitus (T2DM), dyslipidemia, hypertension (HTN), chronic hepatic disease (CHD), and cardiovascular disease (CVD), was obtained by reviewing medical records. Any instances of major surgery or cancer treatment within 5 years prior to health screening were documented. For female patients, menopausal status was recorded. Laboratory values

obtained during the health screening were also documented for each patient, including complete blood count (leukocyte, hemoglobin, platelet), blood urea nitrogen, thyroid function (thyroid stimulating hormone, free thyroxine), blood glucose, glycosylated hemoglobin, triglycerides,  $\gamma$ -glutamyl transferase, high-density lipoprotein, low-density lipoproteins, and total cholesterol.

### PET/CT Imaging protocol and analysis

PET/CT was performed using a dedicated PET/CT system (Gemini TF, Philips Healthcare, Cleveland, OH, USA). Patients were instructed to fast for at least 6 hours prior to their examination, and the fasting status of the patient was verified by blood glucose levels ( $<140 \text{ mg}/\text{dL}$ ). Body weight and height were also recorded prior to imaging. Intravenous injection of F-18-fluorodeoxyglucose ( $5.18 \text{ MBq}/\text{kg}$ ) was administered, and 1 hour later, CT images (80 mA and 140 kVp) were acquired from the vertex to the mid-thigh, using a section thickness of 5 mm. Non-enhanced CT images were reconstructed at a  $512 \times 512$  matrix size and a 50 cm field-of-view. For PET imaging, scans were conducted from the mid-thigh to the vertex, utilizing a  $128 \times 128$  matrix size. Reconstruction of PET images involved the application of the ordered subset expectation maximum iterative reconstruction algorithm. Post-processing steps included the implementation of an 8 mm Gaussian filter and a field-of-view spanning 50 cm.

The open-source 32-bit version 5.8.5 of OsiriX (Pixmeo SARL, Geneva, Switzerland) was employed to analyze the PET/CT DICOM files. The software was accessed via the official website (<http://www.osirix-viewer.com>) on a Mac computer running macOS Ventura 13.2 (Apple Inc., Cupertino, CA, USA). Manual placement of the region-of-interest (ROI) was performed on each image to quantify the area (in  $\text{cm}^2$ ) and of the muscle, VAT, SAT, and peri-meter of the abdomen; the perimeter (in cm) of the abdominal cavity at the level of the umbilicus; and the standardized uptake values (SUV), and Hounsfield unit (HU) measurements of skeletal muscle, adipose tissue, and bone density. The Grow Region (2D/3D segmentation) tool which uses a growing region algorithm was employed for semi-automated selection of skeletal muscle and adipose tissue regions based on preset HU intensity thresholds [11,12]. After which, the brush option within the software was employed to manually exclude non-target tissue regions adjacent to the targets. Automatic computation was employed to express the area of each ROI, the perimeter of the ROI, and to provide mean,



maximum, and minimum values for the HU and SUV.

### Measurements of body composition parameters

For each patient, the amount and distribution of abdominal fat was measured using an axial image showing the transverse process of the fourth lumbar vertebra (L4) as a landmark. Fat tissue falling within the predefined HU range for adipose tissue [13] was identified. VAT was defined as fat located within the visceral cavity. SAT was defined as fat located outside the visceral cavity, excluding any fat located within the muscular fascia or cutaneous tissue (Fig. 1). WC was measured by outlining an ROI along the cutaneous area at the level of the umbilicus.

Cross-sectional muscle area (CSMA) was measured using an axial image showing the transverse processes of the third lumbar vertebra (L3) as a landmark. The image included the psoas, paraspinal, transverse abdominis, external oblique, in-

ternal oblique, and rectus abdominis muscles (Fig. 1C). CSMA (in  $\text{cm}^2$ ) within the specified HU range for muscle tissue [14,15] was identified. The mean HU value within the ROI was also calculated. In addition, a circular ROI with a 1 cm diameter was positioned within the psoas muscle to assess glucose metabolism (Fig. 1D) [16]. To validate the parameter, CSMA was compared with the standardized skeletal muscle index (SMI) obtained by bioelectrical impedance analysis (BIA).

The measurement of HU values was used to estimate fat content in the target organs, as fat typically has low HU values in the range of  $-30$  to  $-190$  [17,18]. A decrease in HU values indicates a higher proportion of voxels within the organ with densities consistent with adipose tissue, thus indicating an increase in fat content. Low HU values have been shown to correlate significantly with intracellular lipid accumulation in organs such as muscle [19] and liver [20].

BMD was determined by measuring the HU at the center of

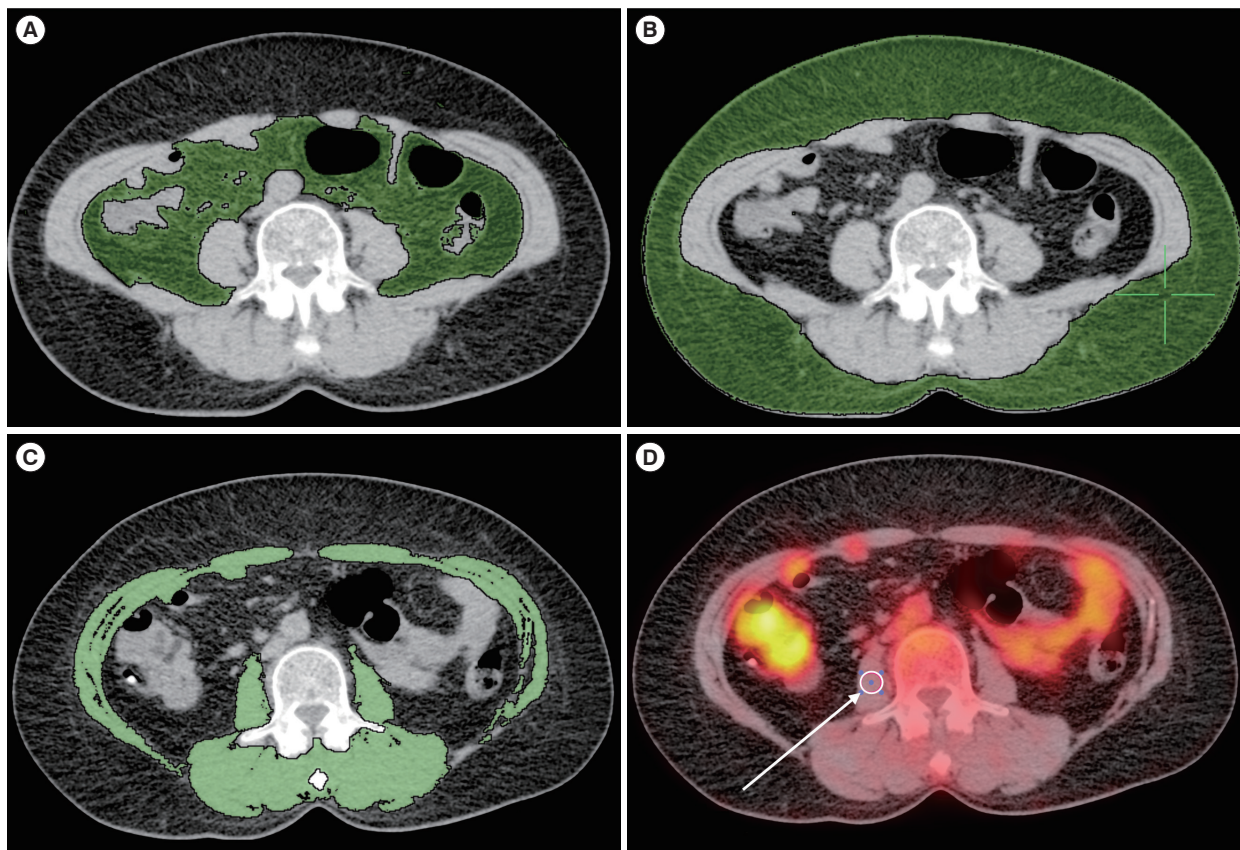


**Fig. 1.** Measurement of body composition parameters. (A) Abdominal visceral adipose tissue and (B) abdominal subcutaneous adipose tissue show in an axial image using the transverse process of the fourth lumbar vertebra. (C) Cross-sectional muscle area and (D) circular region-of-interest with a 1 cm diameter within the psoas muscle (white arrow) shown in an axial image using the transverse processes of the third lumbar vertebra.

either the first (L1) or second (L2) lumbar vertebral body (VB) [1]. To establish the ROI, an oval shape was selected on the axial image, maximizing the circle diameter, while excluding the vertebral cortex and posterior venous plexus. Vertebrae with bone lesions such as hemangiomas, sclerosing foci, or vertebral collapse were excluded from ROI placement. In which cases, comparable measurements were performed on sagittal images using the mid-sagittal section of the L1 or L2 vertebral bodies. All measurements were performed on bone windows, facilitating a more precise detection of bone lesions and any deviations from the characteristic spongy texture of the vertebrae. To validate our findings, the obtained BMD values were compared with areal BMD (aBMD) values derived from dual-energy X-ray absorptiometry (DXA).

To quantify liver fat, an oval-shaped ROI with an average area ranging from 10 to 15 cm<sup>2</sup> was positioned within the liver. The ROI was placed within a representative parenchymal region of the right hepatic lobe, avoiding vessels, focal nodules, masses, and any other sources of heterogeneity. The placement of the ROI was replicated three times, and the resulting mean value was adopted for subsequent analysis. The diagnostic criteria for detecting steatosis on non-contrast CT scans stipulates absolute liver attenuation of less than 40 HU [21]. To validate the parameter, liver HU was compared with the degree of liver brightening and/or blurring of vessels and by liver sonography [22]. Liver HU was also compared with the fatty liver index (FLI) [23,24].

### DXA and BIA

Lumbar aBMD (L1–4) was measured on DXA scans (Lunar Prodigy, GE Medical Systems, Milwaukee, WI, USA) and analyzed using Encore software version 18.0 (GE Healthcare, Madison, WI, USA). T-score was defined as the standard deviation from the mean aBMD of a reference group from the general population, matched for sex and aged between 25 and 35 years. BIA was conducted using the InBody720 and InBody770 (Biospace, Seoul, Korea) body composition analyzer, employing a multifrequency bioimpedance technique. During the procedure, all patients stood with their feet shoulder width apart with the arms abducted slightly from the torso. The feet were then centered on one set of electrodes and another set of electrodes were grasped in the hands.

### Statistical analysis

We investigated the connection between age and body compo-

sition parameters using Pearson's correlation coefficients and linear regression analysis. Additionally, we performed correlation analyses among the body composition parameters. Fisher's Z-transformation was used to evaluate and compare the correlations. Two groups were compared using the independent *t*-test for continuous values and chi-square test for categorical values. Comparisons of two different parameters belonging to a single individual were performed using paired sample *t*-test. We considered a *P* value of 0.05 as indicative of statistical significance. All statistical analyses were performed using R version 4.0.2 software (R Foundation for Statistical Computing, Vienna, Austria).

### Ethics statement

This study was approved by the Institutional Review Board of Seoul Metropolitan Government Seoul National University Boramae Medical Center where the health screening took place (reference no. 10-2021-84), and a waiver of informed of consent was granted due to the retrospective nature of the study.

## RESULTS

### Demographics

A total of 278 patients were included in the study, comprising 140 male and 138 female. While there were no significant difference between sexes in any baseline characteristics, female were slightly older than male ( $62.09 \pm 10.01$  vs.  $59.34 \pm 9.63$  re-

Table 1. Baseline characteristics

Characteristic	Male	Female	<i>P</i> value
Number	140	138	
Age, yr	$59.34 \pm 9.63$	$62.09 \pm 10.01$	0.0313
BMI, kg/m <sup>2</sup>	$24.67 \pm 2.97$	$23.51 \pm 2.84$	0.0010
WC, cm	$85.55 \pm 8.88$	$82.79 \pm 7.86$	0.0066
Abdominal obesity	43 (31.2)	47 (33.6)	0.5514
T2DM	28 (20.3)	19 (13.6)	0.1657
HTN	57 (41.3)	47 (33.6)	0.2825
Dyslipidemia	44 (31.9)	50 (35.7)	0.3973
CHD	4 (2.9)	2 (1.4)	0.6635
CVD	8 (5.8)	3 (2.1)	0.1300
Cancer history	6 (4.3)	6 (4.3)	0.9797

Values are presented as mean  $\pm$  standard deviation or number (%). BMI, body mass index; WC, waist circumference; T2DM, type 2 diabetes mellitus; HTN, hypertension; CHD, chronic hepatic disease; CVD, cardiovascular disease.

spectively;  $P=0.0313$ ), and had numerically less T2DM, HTN, CHD, and CVD. The majority of female patients had experienced menopause ( $n=122/138$ ). Descriptive characteristics of the study patients are summarized in Table 1.

#### Validation of body composition parameters

Body composition parameters obtained by FDG-PET/CT were validated against the established gold standards (Supplementary Figs. 1 and 2). BMD in the L1 VB showed a significant association with aBMD determined by DXA of the L1–L4 region ( $r=0.563$ ,  $P<0.0001$ ). CSMA quantification showed a robust

correlation with SMI acquired by BIA ( $r=0.902$ ,  $P<0.0001$ ). In addition, liver HU on non-enhanced CT scans was associated with the severity of fatty liver as determined by abdominal ultrasonography ( $P=0.0026$ ), and inversely correlated with the FLI ( $r=-0.355$ ,  $P<0.0001$ ).

#### Age-related body composition changes including sex-specific differences

In the total population, age-related changes in body composition showed significant a positive relationship with VAT ( $r=0.222$ ,  $P<0.001$ ); and negative relationships with CSMA ( $r=$

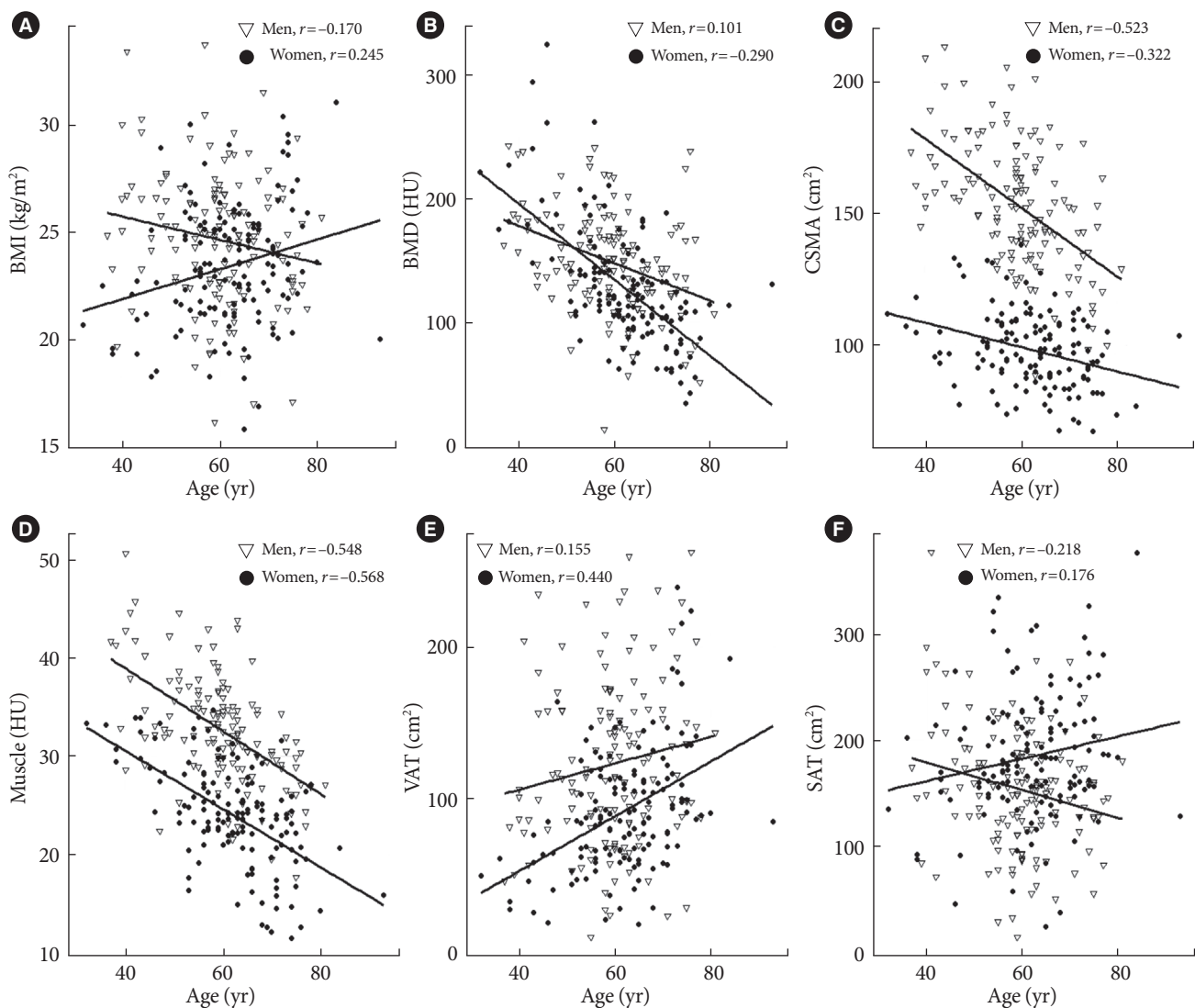


**Fig. 2.** Age-related in body composition changes by sex. Age-related changes analyzed by (A) body mass index (BMI), (B) Hounsfield unit (HU) values for bone mineral density (BMD), (C) cross-sectional muscle area (CSMA), (D) muscle HU values, amounts of (E) abdominal visceral adipose tissue (VAT), and (F) abdominal subcutaneous adipose tissue (SAT).

$-0.355$ ,  $P<0.001$ ), BMD ( $r=-0.1437$ ,  $P=0.0252$ ), and muscle HU ( $r=-0.511$ ,  $P<0.001$ ). Importantly, age-related changes in body composition differed significantly by sex (Fig. 2). Age-related changes in BMI were significantly different between the sexes. In female, there was a significant positive correlation between age and BMI, indicating an increase in BMI over time ( $r=0.245$ ,  $P=0.0038$ ). Conversely, a significant negative correlation between age and BMI was observed in male, suggesting

a slight decrease in BMI with age ( $r=-0.170$ ,  $P=0.044$ ). While BMD showed a significant decrease with age in both female and male, the trend was more pronounced in female ( $r=-0.290$ ,  $P<0.0001$ ) compared to male ( $r=0.101$ ,  $P=0.243$ ), with a significant difference between the sexes ( $P=0.002$ ). Again, CSMA showed significant decrease in age in both male and female, but the trend was greater in male ( $r=-0.523$ ,  $P<0.0001$ ) than in female ( $r=-0.322$ ,  $P=0.0001$ ), with statistical significance

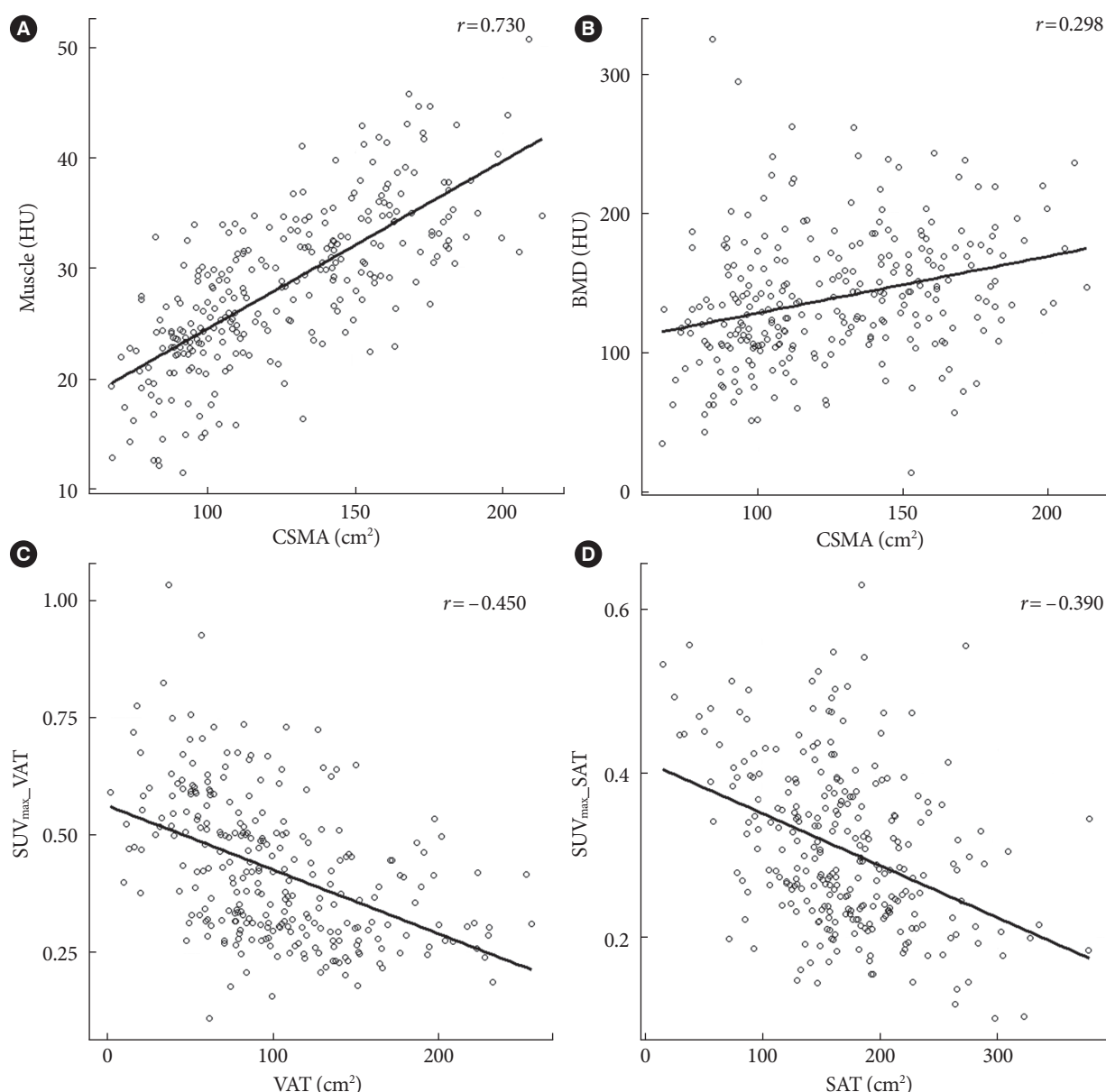


**Fig. 3.** Correlations among body composition parameters. Correlations of cross-sectional muscle area (CSMA) with Hounsfield unit (HU) values of muscle (A) and bone mineral density (BMD) (B). Correlation of glucose metabolism, measured as the maximum correlation of glucose metabolism, measured as the maximum standardized uptake value ( $SUV_{max}$ ), with the amount of (C) abdominal visceral adiposes tissue (VAT), and (D) abdominal subcutaneous adiposes tissue (SAT).



( $P=0.041$ ). In contrast, the significant decline in muscle HU values in both male ( $r=-0.548$ ,  $P<0.0001$ ) and female ( $r=-0.568$ ,  $P<0.0001$ ) were not statistically different between the sexes ( $P=0.812$ ).

Age-related changes in mass of both SAT and VAT were significantly different between sexes. In female, the mass of both SAT and VAT significantly increased with age ( $r=0.176$ ,  $P=0.039$ ;  $r=0.440$ ,  $P<0.001$ , respectively); while in male, SAT demonstrated a marginal but significant decline ( $r=-0.218$ ,  $P=0.010$ ),

while VAT remained relatively stable. Muscle glucose metabolism did not show a significant association with age in male; however, in female it showed a significant increase with age ( $r=0.346$ ,  $P<0.001$ ), showing clear significant differences between sexes (Supplementary Fig. 3A). Statistical results are summarized in Supplementary Table 1.

### Correlations among body composition parameters

The correlations among various parameters obtained through

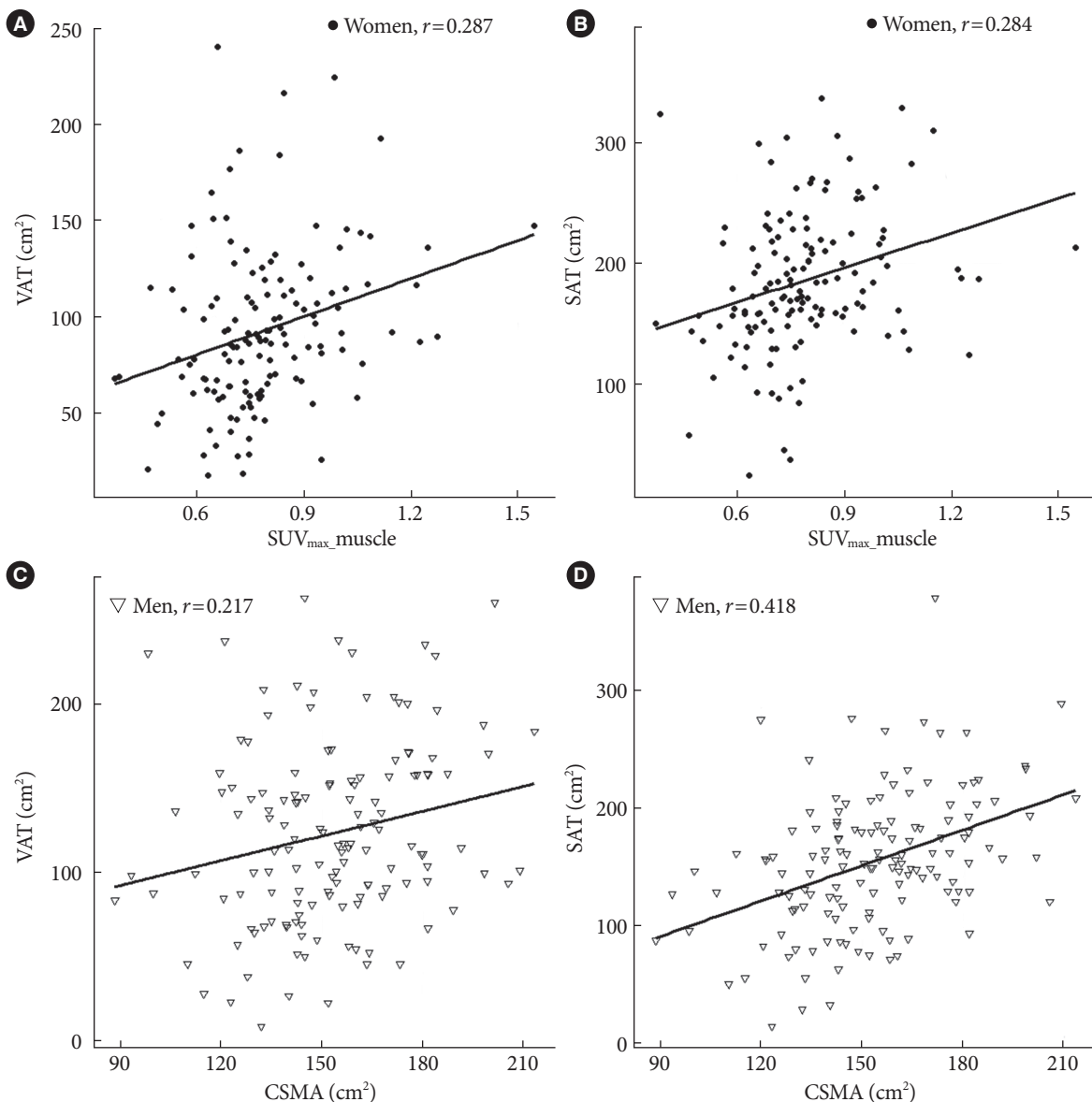


**Fig. 4.** Correlations between fat-related parameters and muscle-related parameters. Correlations of muscle glucose metabolism, measured as the maximum standardized uptake value (SUV<sub>max</sub>), with (A) visceral adipose tissue (VAT) and (B) abdominal subcutaneous adipose tissue (SAT) in female. Correlation of cross-sectional muscle area (CSMA) with (C) VAT and (D) abdominal SAT in male.



PET/CT for body composition analysis were investigated (Fig. 3). Muscle quality, which indicated the amount of fat in the muscle assessed by muscle HU values, exhibited a robust and positive correlation with muscle quantity presented as CSMA ( $r=0.73$ ,  $P<0.0001$ ). CSMA exhibited a significant positive correlation with BMD ( $r=0.298$ ,  $P<0.0001$ ). Both VAT and SAT were significantly negatively correlated with glucose metabolism ( $r=-0.45$ ,  $P<0.001$ ;  $r=-0.39$ ,  $P<0.001$ , respectively). While the glucose metabolism of VAT was higher than that of SAT ( $0.43\pm0.15$  vs.  $0.31\pm0.10$ , respectively;  $P<0.0001$ ), the glucose metabolism of SAT and VAT were positively correlated with each other ( $r=0.733$ ,  $P<0.0001$ ). Interestingly, the amount of both VAT ( $r=0.287$ ,  $P=0.0006$ ) and SAT ( $r=0.284$ ,  $P=0.0007$ ) was positively correlated with muscle glucose metabolism only in female. Conversely, both VAT ( $r=0.217$ ,  $P=0.010$ ) and SAT ( $r=0.418$ ,  $P<0.0001$ ) fat mass were positively correlated with CSMA only in male (Fig. 4). VAT showed a significant inverse relationship with liver HU values, indicating increased fat content of the liver, with a more pronounced correlation shown in female ( $r=-0.501$ ,  $P<0.00001$ ) than male ( $r=-0.387$ ,  $P<0.0001$ ). In addition, VAT showed a significant inverse correlation with muscle HU, indicating increased fat in the muscle, only in female ( $r=-0.268$ ,  $P=0.0015$ ) (Supplementary Fig. 3B). The statistical results are summarized in Supplementary Tables 2 and

3. Fig. 5 shows a correlation heatmap which illustrates the relationships between multiple variables for each sex.

### Subgroup analysis

Subgroups of patients with and without fatty liver, and those with and without T2DM were analyzed. First, patients were dichotomized based on the presence ( $n=100$ ) or absence ( $n=177$ ) of fatty liver. The fatty liver group was older and had a higher BMI and WC than the non-fatty liver group. Additionally, the fatty liver group exhibited higher volumes of VAT and SAT, and showed a significant reduction in glucose metabolism for both SAT and VAT. There were no significant differences in CSMA and muscle HU values between the two groups. However, muscle glucose metabolism was increased in the fatty liver group.

Next, patients were dichotomized based on their T2DM status. The T2DM group ( $n=47$ ) were older and had higher BMI, WC, more VAT, and lower liver HU levels compared to the non-T2DM group ( $n=231$ ). However, there were no differences in other fat-related parameters (amount of SAT and fat glucose metabolism) or muscle-related parameters (CSMA, muscle HU values, and muscle glucose metabolism). The statistical results are summarized in Supplementary Tables 4 and 5.

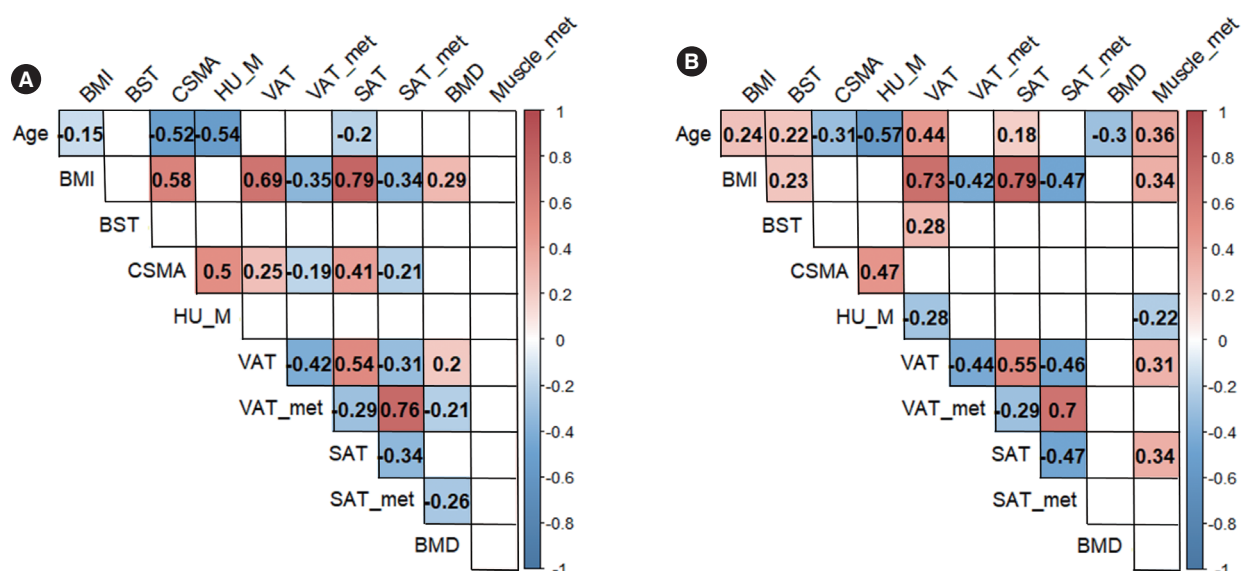


**Fig. 5.** Correlations among body composition parameters. Correlations among body composition parameters in (A) male and (B) female presented as a heatmap. BMI, body mass index; BST, blood sugar test; CSMA, cross-sectional muscle area; HU\_M, Hounsfield unit (HU) of muscle; VAT, amounts of visceral adipose tissue; VAT\_met, maximum standardized uptake value ( $SUV_{max}$ ) of visceral adipose tissue; SAT, amounts of subcutaneous adipose tissue; SAT\_met,  $SUV_{max}$  of subcutaneous adipose tissue; BMD, bone mineral density; Muscle\_met,  $SUV_{max}$  of muscle.

## DISCUSSION

### Age-related body composition change

Our study confirmed distinct patterns of age-related changes in BMI, with notable sex differences. In female, there was a positive correlation between age and BMI, while in male, a weak negative association was observed. It's important to note that BMI is influenced by several factors, including body fat, muscle mass, bone density, and overall body composition. Within this context, we found that both BMD and CSMA decreased with age, and that these parameters were positively correlated; however, the rate of decline differed between the sexes. Specifically, the decrease in CSMA was more pronounced in male than in female, while the decrease in BMD was more pronounced in female than male. These differences may arise from the fact that osteoporosis and sarcopenia develop at different ages and rates between the sexes: female typically begin to lose bone density at an earlier age and at a faster rate than male. While in both sexes, muscle mass tends to decline gradually after the age of 40, and significantly after the age of 50, having peaked in early adulthood [25], the rate of muscle mass loss during aging is typically higher in male than in female [26]. In our study, most female patients had already reached menopause, and the male patients were slightly younger than their female counterparts. The physiological sex-specific age-related differences in the development of sarcopenia and osteopenia may explain the divergence between the sexes in the slopes of the decline in muscle mass and bone density.

We also observed significant sex-based differences in fat mass and distribution with age. In female, both SAT and VAT quantities increased with age. Conversely, in male, SAT decreased slightly while VAT remained relatively stable. Unexpectedly, both VAT and SAT quantities showed a weak positive association with muscle mass, but only in male. This finding seems to contradict the concept of sarcopenic obesity, which is characterized in the elderly by high body fat and low skeletal muscle mass [27]. Rather, the results of the current study suggest that both muscle mass and adipose tissue decrease together in older male, considering the age distribution of male patients ( $59.34 \pm 9.63$  years). A positive correlation between SAT and age has been reported in male aged 20 to 50 years, but this trend was not observed in older male [28].

Our study demonstrated an age-related decline in both muscle mass and muscle quality, and a positive correlation between these parameters. Notably, the rate of decline in muscle mass

was greater in male than in female, whereas the rate of decline in muscle quality was comparable between sexes. Decrease in muscle quality was also evident in patients with fatty liver, although there was no significant difference in muscle mass between the fatty liver and non-fatty liver groups on subgroup analysis. There are two plausible explanations: decreased muscle quality may precede or mask age-related decline in muscle mass, or the method used to select the ROI may have contributed to our results. It has been reported that including intermuscular fat in the ROI results in a more pronounced decrease in mean HU values with age in both sexes compared to muscle mass measurements that exclude intermuscular fat within the ROI [29].

Both our subgroup analyses also demonstrated associations with ectopic fat accumulation and metabolic diseases. The fatty liver group had increased BMI and WC, and showed higher quantities of both VAT and SAT. Patients with T2DM were characterized by increased BMI and WC, and decreased liver HU levels. This suggests that patients with T2DM had a greater accumulation of ectopic fat in the liver, and increased amount of VAT. However, the analyses for both fatty liver and T2DM subgroups failed to show differences in several parameters, including muscle fat content. This may be owing to limited statistical power due to the low number of patients within each of the subgroups.

### Glucose metabolism

Muscle glucose metabolism and fat glucose metabolism showed associations with the amount and distribution of fat in the body. First, muscle glucose metabolism increased significantly with age in female. Moreover, only female exhibited a positive correlation between muscle glucose metabolism and the amount of both VAT and SAT. In addition, an inverse relationship was observed between muscle glucose metabolism and liver HU levels in female only, suggesting that an increase in muscle glucose metabolism may be associated with elevated liver fat content. These findings align with the results of our fatty liver subgroup analysis. Individuals with fatty liver demonstrated increased muscle glucose metabolism. In the total population, fat glucose metabolism was negatively correlated with both VAT and SAT fat mass. These findings are consistent with previous reports of an inverse relationship between fat glucose metabolism and the amount of fat [30-32]. In addition, our results show that, compared to those without fatty liver, individuals with fatty liver had decreased glucose metabolism in both SAT and

VAT. Although not statistically significant, individuals with T2DM also showed a tendency of decreased glucose metabolism in both SAT and VAT. A recent study in patients with T2DM demonstrated a positive correlation between glucose metabolism in VAT and adiponectin levels, and a negative correlation between glucose metabolism in VAT and insulin resistance (IR) [32]. Our results indicate that decreased glucose metabolism in abdominal adipose tissue may be associated with IR, which is closely associated with metabolic diseases such as T2DM and fatty liver disease [33].

### Insulin resistance

Our study provides insights into the correlation between IR and glucose metabolism in muscle, liver, and adipose tissues among individuals with metabolic disease. Previous research has indicated that IR selectively occurs in these tissues, and it has been suggested that IR may occur early in the progression of metabolic disease in the liver and muscle [34]. At the molecular level, IR is characterized by the impaired ability of insulin to activate glucose transport into muscle and adipose cells due to a failure of the glucose transporter protein type-4. Studies involving first-degree relatives of individuals with T2DM report that IR was apparent in both liver and muscle (and potentially adipose tissue) even in the early stage of the disease [35,36]. A similar study showed higher levels of circulating free fatty acids and intramuscular lipids among first-degree relatives of individuals with T2DM compared to healthy control individuals [37]. This indicates that abnormal lipid accumulation may have a greater impact on IR than total obesity.

Our study demonstrated an increase in muscle glucose metabolism in individuals with fatty liver and those with T2DM. Our findings are consistent with a previous study that reported higher glucose uptake in the muscles of diabetic individuals compared to non-diabetic individuals [38]. Furthermore, FDG uptake was increased in the hindlimb skeletal muscle of hyperglycemic mice during fasting conditions without insulin stimulation [39]. Taken together, this demonstrates an accelerated rate of FDG accumulation in diabetics, despite competition from high serum levels of unlabeled glucose. However, there are numerous reports in the literature which contradict this inference [40,41]. For example, it has been reported that in subjects with IR and T2DM, delayed insulin action and glucose uptake results in decreased total glucose uptake by skeletal muscle [40]. Nonetheless, we note that most of these contradictory studies used the hyperinsulinemic-euglycemic clamping

maneuver to estimate impairment in glucose transport or phosphorylation under steadily elevated serum insulin stimulation [40,41]. Thus, our results suggest that various metabolic changes may contribute to the increased glucose metabolism in diabetic subjects under fasting conditions in the absence of insulin stimulation.

We also observed increased fat content in the liver and abdomen, was associated with an increase in muscle glucose metabolism, specifically in female. Notably, there may be sex-based variations in the regulation of insulin-mediated muscle nutrient uptake [42]. Previous studies have demonstrated greater insulin-stimulated whole-body [43] and leg [44] glucose disposal in female than male, despite comparable activation of muscle insulin signaling [44]. Sex-related differences in muscle fiber composition may provide one explanation for the disparities in muscle insulin action between males and females. Specifically, female tend to have a greater relative area of type I fibers, which have a higher capacity for insulin-stimulated glucose metabolism [45], in their skeletal muscle compared to male [46].

### Other considerations

We further investigated the potential confounding effects of comorbidities on age-related changes in body composition and organ-specific glucose metabolism. In male, diabetes mellitus (DM), HTN, dyslipidemia, and CVD were significantly associated with age, and in female, DM and the presence of fatty liver exhibited significance in univariate analysis. Upon controlling for these factors, the results regarding age- and sex-specific changes in body composition and organ-specific glucose metabolism remained unchanged in the multivariate analyses in male.

Additionally, we examined the impact of menopausal status in female. Unfortunately, the multivariate analysis conducted after accounting for menopause did not reveal significant results among the female participants. This could potentially be attributed to the demographic makeup of the female cohort, where the majority were already in the menopausal stage ( $n = 122/138$ ), possibly rendering the control for menopausal status statistically unreliable.

With aging, both male and female experiences in endocrine system such as andropause, menopause, and somatopause [47]. These changes in hormones leads to lifestyle changes, metabolic changes and body composition in aged people. Genome wide associations studies have revealed genetic risk factors also affect functions and composition of our metabolic organs [48].

### Study limitations

The clinical use of systematic opportunistic imaging data is still in its infancy. As such, there are some issues of reproducibility and standardization of imaging acquisition protocols across different settings [2]. There are also various technical (e.g., CT voltage and current settings, and use of contrast/no contrast) and patient-related (e.g., oncologic/non-oncologic and anatomic region) factors which heavily influence the outcomes of opportunistic imaging. The current study was retrospectively conducted, and medication information concerning underlying medical conditions was obtained by reviewing medical records. Although FDG-PET/CT scanning strictly prohibited the use of insulin and medications directly affecting glucose metabolism, factors influencing insulin levels and IR, such as diabetes or metabolic disorders, could still potentially impact glucose metabolism within tissues. Considering that those who undergo health screening may represent individuals who take better care of their health than the general population, our study population, which comprised middle-aged or older individuals who underwent health screening may have influenced our results. Additionally, the small sample size included in this study, especially in the subgroup analyses, may have limited the statistical power of our results. Consequently, some associations may not have achieved clinical significance, potentially affecting the strength of our findings. Nonetheless, the results of our study offer valuable insights into age-related body composition and metabolic changes which may contribute new perspectives for enhancing aging-well and quality of life in older individuals.

In conclusion, body composition analysis using FDG-PET/CT revealed distinct patterns of age-related changes in bone density, muscle mass, fat content, and glucose metabolism, with substantial differences between sexes. Each body composition parameter was interrelated and closely associated with the aging process. Glucose metabolism is intricately linked with both the quantity and distribution of fat, which are influenced by metabolic conditions. In this regard, opportunistic FDG-PET/CT imaging data may provide a more precise evaluation of health risks associated with aging.

### SUPPLEMENTARY MATERIALS

Supplementary materials related to this article can be found online at <https://doi.org/10.4093/dmj.2024.0057>.

### CONFLICTS OF INTEREST

No potential conflict of interest relevant to this article was reported.

### AUTHOR CONTRIBUTIONS

Conception or design: J.I.B., S.W.O.

Acquisition, analysis, or interpretation of data: all authors.

Drafting the work or revising: C.M.O., J.I.B., S.W.O.

Final approval of the manuscript: all authors.

### ORCID

Chang-Myung Oh <https://orcid.org/0000-0001-6681-4478>

Ji-In Bang <https://orcid.org/0000-0003-2962-3642>

So Won Oh <https://orcid.org/0000-0001-8967-8923>

### FUNDING

This research was supported by the Basic Science Research Program through the National Research Foundation of Korea funded by the Ministry of Education (2020R1C1C1004999), and by a National Research Council of Science & Technology (NST) grant by the Korean government (MSIT) (No. CAP23021-000).

### ACKNOWLEDGMENTS

None

### REFERENCES

1. Pickhardt PJ, Graffy PM, Perez AA, Lubner MG, Elton DC, Summers RM. Opportunistic screening at abdominal CT: use of automated body composition biomarkers for added cardiometabolic value. *Radiographics* 2021;41:524-42.
2. Pickhardt PJ. Value-added opportunistic CT screening: state of the art. *Radiology* 2022;303:241-54.
3. Pickhardt PJ, Pooler BD, Lauder T, del Rio AM, Bruce RJ, Binkley N. Opportunistic screening for osteoporosis using abdominal computed tomography scans obtained for other indications. *Ann Intern Med* 2013;158:588-95.
4. Boutin RD, Lenchik L. Value-added opportunistic CT: insights into osteoporosis and sarcopenia. *AJR Am J Roentgenol* 2020;



- 215:582-94.
5. Greco EA, Pietschmann P, Migliaccio S. Osteoporosis and sarcopenia increase frailty syndrome in the elderly. *Front Endocrinol (Lausanne)* 2019;10:255.
  6. Ponti F, Santoro A, Mercatelli D, Gasperini C, Conte M, Martucci M, et al. Aging and imaging assessment of body composition: from fat to facts. *Front Endocrinol (Lausanne)* 2020;10:861.
  7. Netuveli G, Wiggins RD, Hildon Z, Montgomery SM, Blane D. Quality of life at older ages: evidence from the English longitudinal study of aging (wave 1). *J Epidemiol Community Health* 2006;60:357-63.
  8. Brett CE, Dykiert D, Starr JM, Deary IJ. Predicting change in quality of life from age 79 to 90 in the Lothian Birth Cohort 1921. *Qual Life Res* 2019;28:737-49.
  9. Rudnicka E, Napierala P, Podfigurna A, Meczekalski B, Smolarczyk R, Grymowicz M. The World Health Organization (WHO) approach to healthy ageing. *Maturitas* 2020;139:6-11.
  10. Lee SY, Park HS, Kim DJ, Han JH, Kim SM, Cho GJ, et al. Appropriate waist circumference cutoff points for central obesity in Korean adults. *Diabetes Res Clin Pract* 2007;75:72-80.
  11. Savarino E, Savarino V, Fox M, Di Leo G, Furnari M, Marabotto E, et al. Measurement of oro-caecal transit time by magnetic resonance imaging. *Eur Radiol* 2015;25:1579-87.
  12. Chen KY, Cypess AM, Laughlin MR, Haft CR, Hu HH, Bredella MA, et al. Brown Adipose Reporting Criteria in Imaging Studies (BARCIST 1.0): recommendations for standardized FDG-PET/CT experiments in humans. *Cell Metab* 2016;24:210-22.
  13. Tanaka T, Kishi S, Ninomiya K, Tomii D, Koseki K, Sato Y, et al. Impact of abdominal fat distribution, visceral fat, and subcutaneous fat on coronary plaque scores assessed by 320-row computed tomography coronary angiography. *Atherosclerosis* 2019;287:155-61.
  14. Mourtzakis M, Prado CM, Lieffers JR, Reiman T, McCargar LJ, Baracos VE. A practical and precise approach to quantification of body composition in cancer patients using computed tomography images acquired during routine care. *Appl Physiol Nutr Metab* 2008;33:997-1006.
  15. Prado CM, Lieffers JR, McCargar LJ, Reiman T, Sawyer MB, Martin L, et al. Prevalence and clinical implications of sarcopenic obesity in patients with solid tumours of the respiratory and gastrointestinal tracts: a population-based study. *Lancet Oncol* 2008;9:629-35.
  16. Kim K, Kim IJ, Pak K, Kang T, Seol YM, Choi YJ, et al. Prognostic value of metabolic activity of the psoas muscle evaluated by preoperative 18F-FDG PET-CT in breast cancer: a retrospective cross-sectional study. *BMC Cancer* 2021;21:1151.
  17. Bydder GM, Chapman RW, Harry D, Bassan L, Sherlock S, Kreel L. Computed tomography attenuation values in fatty liver. *J Comput Tomogr* 1981;5:33-5.
  18. Kim S, Lee GH, Lee S, Park SH, Pyo HB, Cho JS. Body fat measurement in computed tomography image. *Biomed Sci Instrum* 1999;35:303-8.
  19. Aubrey J, Esfandiari N, Baracos VE, Buteau FA, Frenette J, Putman CT, et al. Measurement of skeletal muscle radiation attenuation and basis of its biological variation. *Acta Physiol (Oxf)* 2014;210:489-97.
  20. Starekova J, Hernando D, Pickhardt PJ, Reeder SB. Quantification of liver fat content with CT and MRI: state of the art. *Radiology* 2021;301:250-62.
  21. Wells MM, Li Z, Addeman B, McKenzie CA, Mujoomdar A, Beaton M, et al. Computed tomography measurement of hepatic steatosis: prevalence of hepatic steatosis in a Canadian population. *Can J Gastroenterol Hepatol* 2016;2016:4930987.
  22. Zhang YN, Fowler KJ, Hamilton G, Cui JY, Sy EZ, Balanay M, et al. Liver fat imaging-a clinical overview of ultrasound, CT, and MR imaging. *Br J Radiol* 2018;91:20170959.
  23. Bedogni G, Bellentani S, Miglioli L, Masutti F, Passalacqua M, Castiglione A, et al. The fatty liver index: a simple and accurate predictor of hepatic steatosis in the general population. *BMC Gastroenterol* 2006;6:33.
  24. Khang AR, Lee HW, Yi D, Kang YH, Son SM. The fatty liver index, a simple and useful predictor of metabolic syndrome: analysis of the Korea National Health and Nutrition Examination Survey 2010-2011. *Diabetes Metab Syndr Obes* 2019;12:181-90.
  25. Dennison EM, Sayer AA, Cooper C. Epidemiology of sarcopenia and insight into possible therapeutic targets. *Nat Rev Rheumatol* 2017;13:340-7.
  26. Zamboni M, Zoico E, Scartezzini T, Mazzali G, Tosoni P, Zivelonghi A, et al. Body composition changes in stable-weight elderly subjects: the effect of sex. *Aging Clin Exp Res* 2003;15:321-7.
  27. Batsis JA, Villareal DT. Sarcopenic obesity in older adults: aetiology, epidemiology and treatment strategies. *Nat Rev Endocrinol* 2018;14:513-37.
  28. Szulc P, Duboeuf F, Chapurlat R. Age-related changes in fat mass and distribution in men-the cross-sectional STRAMBO Study. *J Clin Densitom* 2017;20:472-9.

29. Graffy PM, Liu J, Pickhardt PJ, Burns JE, Yao J, Summers RM. Deep learning-based muscle segmentation and quantification at abdominal CT: application to a longitudinal adult screening cohort for sarcopenia assessment. *Br J Radiol* 2019;92:20190327.
30. Oliveira AL, Azevedo DC, Bredella MA, Stanley TL, Torriani M. Visceral and subcutaneous adipose tissue FDG uptake by PET/CT in metabolically healthy obese subjects. *Obesity (Silver Spring)* 2015;23:286-9.
31. Goncalves MD, Green-McKenzie J, Alavi A, Torigian DA. Regional variation in skeletal muscle and adipose tissue FDG uptake using PET/CT and their relation to BMI. *Acad Radiol* 2017;24:1288-94.
32. Reijrink M, de Boer SA, Antunes IF, Spoor DS, Heerspink HJL, Lodewijk ME, et al. [18F]FDG uptake in adipose tissue is not related to inflammation in type 2 diabetes mellitus. *Mol Imaging Biol* 2021;23:117-26.
33. Tanase DM, Gosav EM, Costea CF, Ciocoiu M, Lacatusu CM, Maranduca MA, et al. The intricate relationship between type 2 diabetes mellitus (T2DM), insulin resistance (IR), and nonalcoholic fatty liver disease (NAFLD). *J Diabetes Res* 2020;2020:3920196.
34. Tan SX, Fisher-Wellman KH, Fazakerley DJ, Ng Y, Pant H, Li J, et al. Selective insulin resistance in adipocytes. *J Biol Chem* 2015;290:11337-48.
35. Ferrannini E, Gastaldelli A, Matsuda M, Miyazaki Y, Pettiti M, Glass L, et al. Influence of ethnicity and familial diabetes on glucose tolerance and insulin action: a physiological analysis. *J Clin Endocrinol Metab* 2003;88:3251-7.
36. Vaag A, Henriksen JE, Beck-Nielsen H. Decreased insulin activation of glycogen synthase in skeletal muscles in young non-obese Caucasian first-degree relatives of patients with non-insulin-dependent diabetes mellitus. *J Clin Invest* 1992;89:782-8.
37. Jacob S, Machann J, Rett K, Brechtel K, Volk A, Renn W, et al. Association of increased intramyocellular lipid content with insulin resistance in lean nondiabetic offspring of type 2 diabetic subjects. *Diabetes* 1999;48:1113-9.
38. Ferrannini E. A journey in diabetes: from clinical physiology to novel therapeutics: the 2020 Banting Medal for Scientific Achievement Lecture. *Diabetes* 2021;70:338-46.
39. Bauckneht M, Cossu V, Castellani P, Piccioli P, Orenco AM, Emionite L, et al. FDG uptake tracks the oxidative damage in diabetic skeletal muscle: an experimental study. *Mol Metab* 2020;31:98-108.
40. DeFronzo RA, Jacot E, Jequier E, Maeder E, Wahren J, Felber JP. The effect of insulin on the disposal of intravenous glucose: results from indirect calorimetry and hepatic and femoral venous catheterization. *Diabetes* 1981;30:1000-7.
41. Thiebaud D, Jacot E, DeFronzo RA, Maeder E, Jequier E, Felber JP. The effect of graded doses of insulin on total glucose uptake, glucose oxidation, and glucose storage in man. *Diabetes* 1982;31:957-63.
42. Goossens GH, Jocken JW, Blaak EE. Sexual dimorphism in cardiometabolic health: the role of adipose tissue, muscle and liver. *Nat Rev Endocrinol* 2021;17:47-66.
43. Nuutila P, Knuuti MJ, Maki M, Laine H, Ruotsalainen U, Teras M, et al. Gender and insulin sensitivity in the heart and in skeletal muscles: studies using positron emission tomography. *Diabetes* 1995;44:31-6.
44. Hoeg L, Roepstorff C, Thiele M, Richter EA, Wojtaszewski JF, Kiens B. Higher intramuscular triacylglycerol in women does not impair insulin sensitivity and proximal insulin signaling. *J Appl Physiol (1985)* 2009;107:824-31.
45. Albers PH, Pedersen AJ, Birk JB, Kristensen DE, Vind BF, Baba O, et al. Human muscle fiber type-specific insulin signaling: impact of obesity and type 2 diabetes. *Diabetes* 2015;64:485-97.
46. Staron RS, Hagerman FC, Hikida RS, Murray TF, Hostler DP, Crill MT, et al. Fiber type composition of the vastus lateralis muscle of young men and women. *J Histochem Cytochem* 2000;48:623-9.
47. Pataky MW, Young WF, Nair KS. Hormonal and metabolic changes of aging and the influence of lifestyle modifications. *Mayo Clin Proc* 2021;96:788-814.
48. Li X, Qi L. Gene-environment interactions on body fat distribution. *Int J Mol Sci* 2019;20:3690.

Supplementary Table 1. Age-related changes in body composition parameters

Variable	Age													
	Total		Male		Female		Male				Female			
	<i>r</i>	<i>P</i> value	<i>r</i>	<i>P</i> value	<i>r</i>	<i>P</i> value	Slope	Intercept	<i>R</i> <sup>2</sup>	<i>P</i> value	Slope	Intercept	<i>R</i> <sup>2</sup>	<i>P</i> value
CSMA	−0.355	<0.001	−0.523	<0.001	−0.322	<0.001	−1.302	230.423	0.274	<0.001	−0.461	127.020	0.104	<0.001
BMI	0.004	0.955	−0.170	0.044	0.245	0.004	−0.054	27.921	0.029	0.044	0.069	19.121	0.060	0.004
BMD	−0.137	0.025	0.101	0.243	−0.290	0.001	0.002	1.018	0.010	0.243	−0.005	1.304	0.084	<0.001
Muscle_HU	−0.511	<0.001	−0.548	<0.001	−0.568	<0.001	−0.318	51.690	0.300	<0.001	−0.295	42.382	0.322	<0.001
VAT	0.222	<0.001	0.155	0.067	0.440	<0.001	0.869	71.394	0.024	0.067	1.807	−19.872	0.193	<0.001
SAT	0.019	0.750	−0.218	0.010	0.176	0.039	−1.304	231.838	0.047	<0.001	1.056	119.757	0.031	0.039
VAT_SUV <sub>max</sub>	−0.014	0.820	0.121	0.154	−0.164	0.054	0.002	0.302	0.015	0.154	−0.003	0.606	0.027	0.005
SAT_SUV <sub>max</sub>	−0.016	0.793	0.093	0.276	−0.129	0.132	<0.001	0.247	0.009	0.276	−0.001	0.396	0.017	0.132

CSMA, cross-sectional muscle area; BMI, body mass index; BMD, bone mineral density; HU, Hounsfield unit; VAT, visceral adipose tissue; SAT, subcutaneous adipose tissue; SUV<sub>max</sub>, maximum standardized uptake value.

**Supplementary Table 2.** Correlations among body composition parameters related to muscle

Variable	Total		Male		Female		Male				Female			
	<i>r</i>	<i>P</i> value	<i>r</i>	<i>P</i> value	<i>r</i>	<i>P</i> value	Slope	Intercept	<i>R</i> <sup>2</sup>	<i>P</i> value	Slope	Intercept	<i>R</i> <sup>2</sup>	<i>P</i> value
Muscle mass (CSMA)														
BMD	0.395	<0.001	0.146	0.092	0.129	0.142	18.709	131.803	0.021	0.009	9.385	89.124	0.017	0.142
VAT	0.318	<0.001	0.217	0.010	−0.078	0.362	0.097	140.988	0.047	<0.001	−0.027	100.926	0.006	0.362
SAT	−0.085	0.158	0.418	<0.001	−0.090	0.292	0.174	126.114	0.175	<0.001	−0.022	102.408	0.008	0.292
BMI	0.410	<0.001	0.590	<0.001	0.130	0.127	4.604	39.240	0.350	<0.001	0.660	82.957	0.017	0.127
VAT_SUV <sub>max</sub>	−0.167	0.005	−0.176	0.038	−0.010	0.912	−29.930	165.081	0.038	0.031	−0.867	98.800	0.912	<0.001
SAT_SUV <sub>max</sub>	−0.122	0.041	−0.220	0.009	0.040	0.643	−56.863	169.993	0.009	0.048	5.560	96.663	0.643	0.002
Muscle_SUV <sub>max</sub>	−0.225	<0.001	0.030	0.722	−0.051	0.549	<0.001	0.669	0.001	0.722	−0.001	0.851	0.003	0.549
Muscle quality (HU)														
BMD	0.263	<0.001	−0.109	0.211	0.170	0.052	−0.004	1.246	0.012	0.211	0.006	0.825	0.029	0.052
VAT	0.054	0.373	−0.125	0.144	−0.268	0.001	−1.190	161.666	0.016	0.144	−2.120	143.300	0.072	0.001
SAT	−0.151	0.012	0.131	0.125	−0.101	0.241	1.337	109.856	0.017	0.125	−1.161	213.228	0.010	0.241
BMI	0.162	0.007	0.142	0.096	−0.071	0.408	0.077	22.132	0.020	0.096	−0.039	24.355	0.005	0.408
VAT_SUV <sub>max</sub>	−0.028	0.642	0.082	0.338	0.054	0.529	0.002	0.341	0.007	0.338	0.002	0.407	0.003	0.529
SAT_SUV <sub>max</sub>	0.009	0.881	0.028	0.744	0.103	0.229	<0.001	0.286	0.001	0.744	0.002	0.265	0.011	0.229
Muscle_SUV <sub>max</sub>	−0.240	<0.001	0.036	0.672	−0.202	0.017	0.001	0.667	0.001	0.672	−0.007	0.955	0.041	0.017

CSMA, cross-sectional muscle area; BMD, bone mineral density; VAT, visceral adipose tissue; SAT, subcutaneous adipose tissue; BMI, body mass index; SUV<sub>max</sub>, maximum standardized uptake value; HU, Hounsfield unit.



Supplementary Table 3. Correlations among parameters related to amount of fat

Variable	Liver HU													
	Total		Male		Female		Male				Female			
	<i>r</i>	<i>P</i> value	<i>r</i>	<i>P</i> value	<i>r</i>	<i>P</i> value	Slope	Intercept	<i>R</i> <sup>2</sup>	<i>P</i> value	Slope	Intercept	<i>R</i> <sup>2</sup>	<i>P</i> value
BMD	−0.195	0.001	−0.258	0.003	−0.078	0.379	−0.006	1.358	0.066	0.003	−0.002	1.039	0.006	0.379
BMI	−0.417	<0.001	−0.308	<0.001	−0.502	<0.001	−0.110	29.294	0.095	<0.001	−0.154	30.108	0.252	<0.001
VAT	−0.445	<0.001	−0.387	<0.001	−0.501	<0.001	−2.461	224.626	0.150	<0.001	−2.233	189.092	0.251	<0.001
SAT	−0.279	<0.001	−0.267	0.001	−0.376	<0.001	−1.783	226.668	0.071	0.001	−2.446	291.347	0.141	<0.001
VAT_SUV <sub>max</sub>	0.470	<0.001	0.450	<0.001	0.472	<0.001	0.007	0.099	0.202	<0.001	0.008	0.098	0.223	<0.001
SAT_SUV <sub>max</sub>	0.447	<0.001	0.404	<0.001	0.476	<0.001	0.004	0.119	0.085	<0.001	0.005	0.085	0.227	<0.001
Muscle_SUV <sub>max</sub>	−0.106	0.078	−0.102	0.233	−0.178	0.037	−0.002	0.765	0.010	0.233	−0.003	0.937	0.032	0.037

HU, Hounsfield unit; BMD, bone mineral density; BMI, body mass index; VAT, visceral adipose tissue; SAT, subcutaneous adipose tissue; SUV<sub>max</sub>, maximum standardized uptake value.

**Supplementary Table 4.** Body composition parameters of patients with and without fatty liver

Variable	Fatty liver group	Non-fatty liver group	P value
Number	100	177	
Age, yr	62.66±10.18	59.79±9.45	0.0195
BMI, kg/m <sup>2</sup>	25.57±2.52	23.24±2.99	<0.0001
WC, cm	88.37±7.37	81.72±8.08	<0.0001
VAT, cm <sup>2</sup>	137.12±45.43	91.25±45.44	<0.0001
VAT_SUV <sub>max</sub>	0.31±0.07	0.49±0.15	<0.0001
SAT, cm <sup>2</sup>	192.57±59.22	156.68±57.29	<0.0001
SAT_SUV <sub>max</sub>	0.24±0.06	0.35±0.10	<0.0001
CSMA, cm <sup>2</sup>	130.69±34.70	122.65±32.34	0.0539
Muscle_HU	27.64±6.97	28.71±6.72	0.2122
Muscle_SUV <sub>max</sub>	0.77±0.20	0.73±0.15	<0.0001

Values are presented as mean ± standard deviation. One patient whose liver could not be evaluated due to severe beam-hardening artifact was excluded.

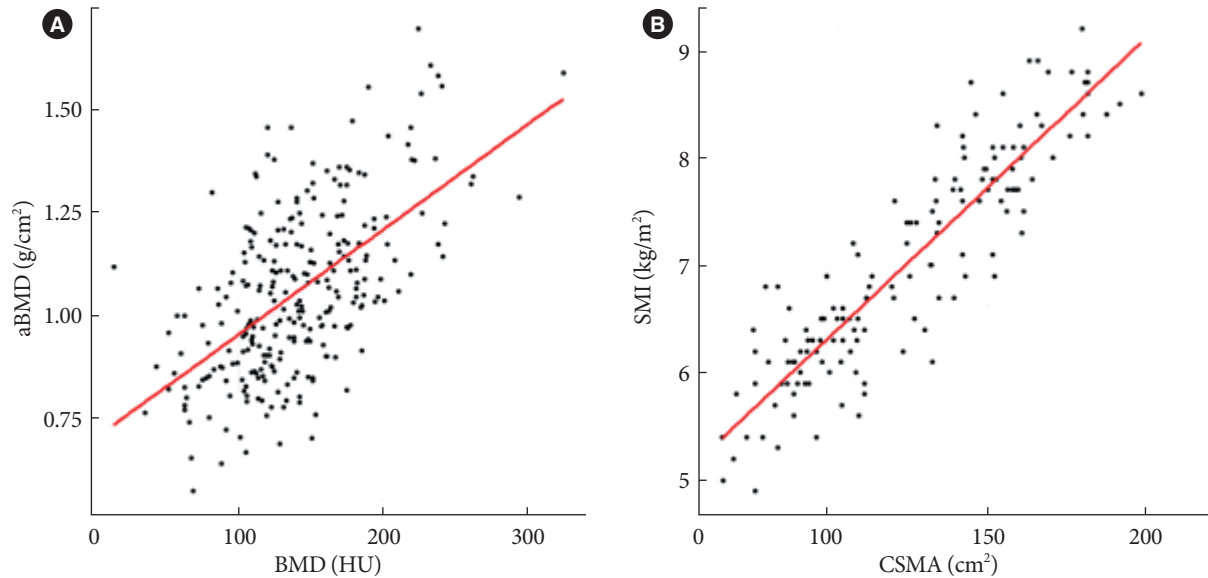
BMI, body mass index; WC, waist circumference; VAT, visceral adipose tissue; SUV<sub>max</sub>, maximum standardized uptake value; SAT, subcutaneous adipose tissue; CSMA, cross-sectional muscle area; HU, Hounsfield unit.

**Supplementary Table 5.** Body composition parameters of patients with and without type 2 diabetes mellitus

Variable	T2DM	Non-T2DM	P value
Number	47	231	
Age, yr	66.70±9.21	59.60±9.61	<0.0001
BMI, kg/m <sup>2</sup>	25.04±3.16	23.86±2.96	0.0217
WC, cm	86.97±8.61	83.61±8.37	0.0172
VAT, cm <sup>2</sup>	138.36±51.72	101.61±47.79	<0.0001
VAT_SUV <sub>max</sub>	0.41±0.14	0.43±0.15	0.3480
SAT, cm <sup>2</sup>	174.51±61.44	168.65±60.79	0.5487
SAT_SUV <sub>max</sub>	0.29±0.08	0.31±0.10	0.1331
CSMA, cm <sup>2</sup>	128.39±34.48	125.33±33.58	0.5712
Muscle_HU	26.61±7.15	28.76±6.86	0.0554
Muscle_SUV <sub>max</sub>	0.78±0.18	0.73±0.16	0.0900
Liver_HU	38.77±8.65	43.19±8.23	0.0021

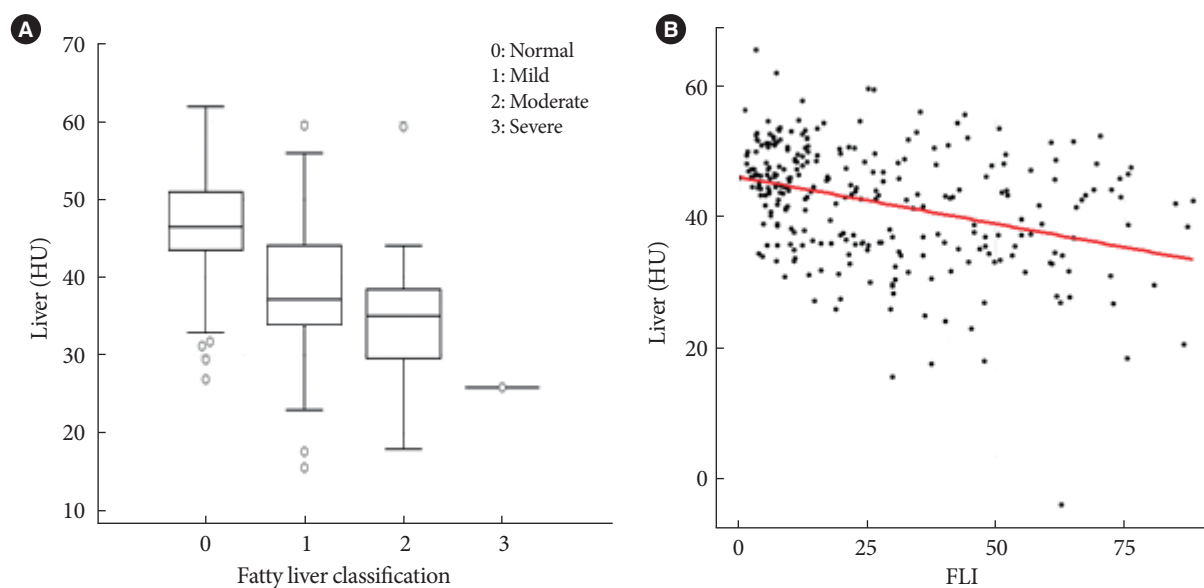
Values are presented as mean ± standard deviation.

T2DM, type 2 diabetes mellitus; BMI, body mass index; WC, waist circumference; VAT, visceral adipose tissue; SUV<sub>max</sub>, maximum standardized uptake value; SAT, subcutaneous adipose tissue; CSMA, cross-sectional muscle area; HU, Hounsfield unit.

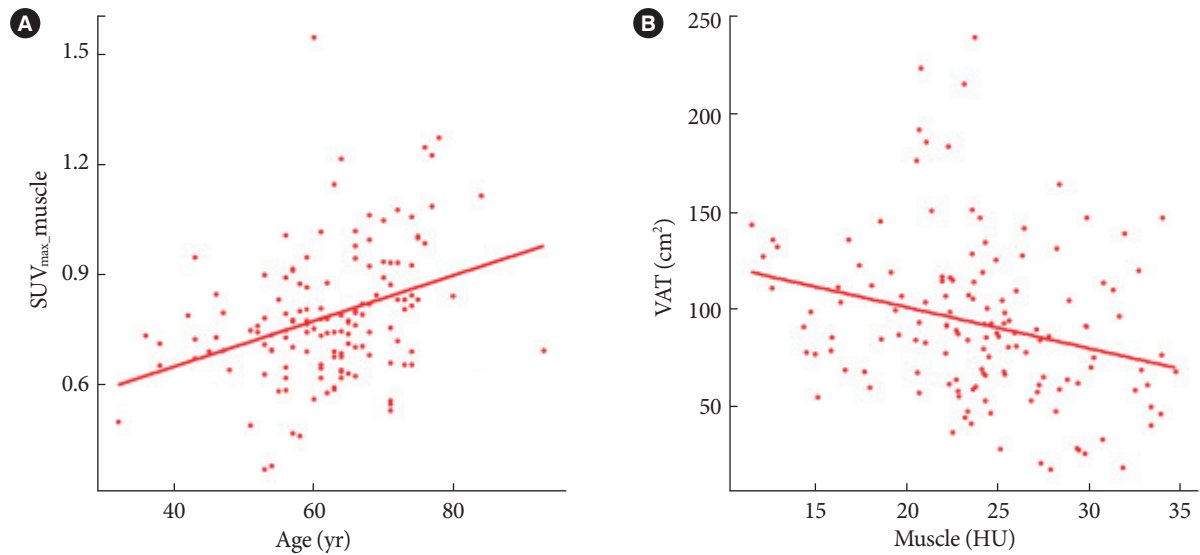


**Supplementary Fig. 1.** Validation of body composition parameters. (A) Evaluation of bone mineral density (BMD) by 18-fluoro-deoxyglucose positron emission tomography/computed tomography shows a significant association with areal BMD (aBMD) determined by dual-energy X-ray absorptiometry, with both measurements using the Hounsfield (HU) unit. (B) Cross-sectional muscle area (CSMA) quantification shows a robust correlation with skeletal muscle index (SMI) acquired by bioelectrical impedance analysis.





**Supplementary Fig. 2.** Validation of body composition parameters. (A) Liver Hounsfield unit (HU) of non-enhanced computed tomography scans shows an association with the severity of fatty liver disease as determined by abdominal ultrasonography. (B) Liver HU value shows an inverse correlation with the fatty liver index (FLI).



**Supplementary Fig. 3.** Correlations of body composition parameters in female only. (A) Muscle glucose metabolism, measured as maximum standardized uptake value ( $SUV_{max}$ ), shows an increase with age. (B) Visceral adipose tissue (VAT) shows an inverse correlation with muscle Hounsfield unit (HU), indicating increased fat in the muscle.